PROGRESS
IN COLOR, COLORANTS AND COATINGS

available online @ www.pccc.icrc.ac.ir

Progress in Color Colorants Coating 16 (2023), 21-29

Ministry of Science, Research and Technology
Institute for Color Science & Technology

Fabrication of Lead Iodide Perovskite Solar Cells by Incorporating Cr-substituted and Pristine $Ba_2In_2O_5{\cdot}(H_2O)_x$ as Additives

M. Seifpanah Sowmehsaraee, M. Ranjbar*, M. Abedi**
Department of Chemical Technologies, Iranian Research Organization for Science and Technology (IROST), P. O. Box: 3353-5111, Tehran, Iran.

ARTICLE INFO

Article history:
Received: 18 Oct 2021
Final Revised: 20 Apr 2022
Accepted: 24 Apr 2022
Available online: 27 Aug 2022

Keywords:
Perovskite solar cells
Additive
$Ba_2In_2O_5{\cdot}(H_2O)_x$
$Ba_2(In_{1.8}Cr_{0.2})\ O_5{\cdot}(H_2O)y$
Solvent engineering technique.

ABSTRACT

In this study, two inorganic additives with perovskite structure have been used as additives in fabrication of perovskite solar cells (PSCs). $Ba_2In_2O_5{\cdot}(H_2O)_x$ and $Ba_2(In_{1.8}Cr_{0.2})O_5{\cdot}(H_2O)_y$ was applied in perovskite precursor solution for synthesis of photo absorption layer in PCSs by a one-step solution method with solvent engineering technique. Cr-substituted and pristine $Ba_2In_2O_5{\cdot}(H_2O)_x$ were prepared by solid-state and soft chemistry methods like the procedures in previous work, and utilized to improve the crystal structure and morphology of perovskite layer of PSCs. The morphology of the new perovskite layers was studied by FE-SEM, and XRD analysis. The results showed using 2 wt % of additives in precursor solution of fabricated PCS_s increased the open-circuit voltage (V_{oc}) of cells, also the power-conversion efficiency of the cells improved from 7.8 % to 9.7, and 9.3 % by using both additives respectively. Cr-substituted and pristine $Ba_2In_2O_5{\cdot}(H_2O)_x$ could modify the coverage of perovskite film on the TiO_2 layer and consequently improve the photovoltaic stability and performance of perovskite solar cells. Prog. Color Colorants Coat. 16 (2023), 21-29© Institute for Color Science and Technology.

1. Introduction

Perovskite solar cells (PSCs) have attracted lots of academic and significant attention due to their exciting properties such as the wide adsorption coefficient, broad adsorption range, long diffusion length, and outstanding charge carrier's mobility [1-4]. The critical issue in PSCs is controlling the morphology of the perovskite layer due to improving the stability and power-conversion efficiency (PCE) of cells [5-7]. For this purpose, various methods proposed, in which that one of this method is adding additive in the perovskite precursor solutions. For example, polymer, metal-halide salts, fullerene, organic halide salts, and inorganic acids were used in perovskite solution [8]. In many types of research, Metal-Organic Frameworks (MOFs) have been used as a kind of applications such as gas storage [9], separation [10], chemical sensing [11], catalysis [12, 13], photocatalysis [14-16].

The significant progress in light-harvesting by MOFs was studied, and evaluated by Wang et al [17]. Recently, MOFs were applied as new additives in PSCs, For example, Vinogradov et al. [18] were applied $Ti_8O_8(OH)_4$-$(O_2C$-C_6H_4-$CO_2)_6$ (MIL-125) in electron transport layer to enhancing the stability of PSCs. So, Wei et al. [19] employed $C_8H_{10}N_4Zn$ (ZIF-8) for improving the crystallization and the photovoltaic

*Corresponding author: * marandjbar@irost.ir
**mabedi@irost.ir
Doi: 10.30509/PCCC.2022.166906.1137

properties of PSCs. Then, Ho et al. [20] applied MOF-525 as additives into the $CH_3NH_3PbI_3$ solution, and reported due to adding MOF-235 in $CH_3NH_3PbI_3$ solution the crystallinity of perovskite layer was improved. Moreover, Li et al. [21] used a 3D MOF $[In_2(phen)_3Cl_6].CH_3CN.2H_2O(In_2)$ as additive into the hole transport materials. In other efforts, they employed this 3D MOF in PbI_2 solution to modify perovskite layer [22]. Ranjbar et al. [23- 27] used Zirconium, Zinc, Indium metal-organic-framework, and MOF-235 as additives into the $CH_3NH_3PbI_3$ solution, and led to a significant increase inefficiency. As a results, MOFs are considered to be a be large additives for apply in PSCs and it is possible to attain optimal result in quality crystallinity and morphology of perovskite film.

In our study, we employed additives with the perovskite structure, which used Metal-Organic Framework (MOFs) in their synthesis were used in perovskite solar cells (PSCs). Cr-substituted and pristine $Ba_2In_2O_5{\cdot}(H_2O)_x$ utilized as new additives in perovskite precursor solution. Cr-substituted and pristine $Ba_2In_2O_5{\cdot}(H_2O)_x$ was first prepared by our group, and Yoon et al. [28]. We proposed $Ba_2In_2O_5{\cdot}(H_2O)_x$ and $Ba_2(In_{1.8}Cr_{0.2})O_5{\cdot}(H_2O)_y$ because MOFs such as $InLH_2$, and $CrLH_2$ are used as precursors in their synthesis. In addition these additives have a perovskite structure, and are expected to be more compatible with $CH_3NH_3PbI_3$.

Then, we choose an anti-solvent technique and a one-step method for fabrication of PSCs because this method achieved a good result in the previous report. [7]. So, at the first time the $Ba_2In_2O_5{\cdot}(H_2O)_x$ and $Ba_2(In_{1.8}Cr_{0.2})O_5{\cdot}(H_2O)_y$ utilized an additive in perovskite solutions to improve the performance of PSCs. The effect of additives on perovskite films shows better morphology. Thus, it provides development in the performance of PSCs. Our discussion mainly focused on the effect of $Ba_2In_2O_5{\cdot}(H_2O)_x$ and $Ba_2(In_{1.8}Cr_{0.2})O_5(H_2O)_y$ in perovskite films and their roles in light absorption, film morphology and performances of devices.

2. Experimental

2.1. Materials and physical techniques

All of materials for the preparation of additives and analysis were commercially obtained from Merck Company. Materials for the fabrication of solar cells such as PbI_2, the TiO_2 paste, CH_3NH_3I, and spiro purchased from Sharif Solar Company.

The Fourier transform infrared (FT-IR) spectra was registered on a Bruker tensor 27 spectrophotometer by using of the KBr disk technique in the range 400–4000 cm^{-1}. The investigation of absorption of perovskite films, UV-Vis spectra were recorded on a Perkin-Elmer, lambada = 25.

The crystalline nature, and phase purity examined using powder X-ray diffraction (XRD) technique (X'Pert Pro, INEL Equinox 3000, X-ray diffractometer) at room temperature with Cu-Kα (λ = 1.54 Å) radiation. The crystallite sizes of perovskite layer were calculated using the Scherrer formula [30]. Tescan Mira FE-SEM, and energy dispersive X-ray (EDX) instrument was used to study the surface morphology of perovskite layers.

Current-voltage (I-V) curves were calculated under simulated sunlight instrument SIM10 model, air mass 1.5 G illumination (palmsens) sharif solar, Iran at 100 mW/cm^2. Impedance spectroscopic measurements were performed using an electrochemical workstation (Autolab 302 N) with the frequency range from (100kHz-100 mHz), scan rate and scan range are 0.1 v/s, (-0.4-0.8), and V_{ocp}= 0.17 V., for cyclic voltammetry (CV).

2.2. Preparation of $Ba_2In_2O_5{\cdot}(H_2O)_x$ and $Ba_2(In_{1.8}Cr_{0.2})O_5{\cdot}(H_2O)_y$ by solid-state and soft chemistry methods

Cr-substituted and pristine $Ba_2In_2O_5{\cdot}(H_2O)_x$ were prepared by the previous report [28]. $Ba_2In_2O_5{\cdot}(H_2O)_x$ and $Ba_2(In_{1.8}Cr_{0.2})O_5{\cdot}(H_2O)_y$ powders by solid-state reactions were synthesized, and prepared. For preparation of additives, $Ba_2In_2O_5{\cdot}(H_2O)_x$, 0.03 mol $BaCO_3$ and 0.015 mol In_2O_3 powder, by using an agate mortar mixed, then were calcined in the air for 12 h at 1173 K, and finally for 12 h at 1473 K with grinding steps. In the following, 0.03 mol $BaCO_3$, 0.0015 mol Cr_2O_3 , and 0.0135 mol In_2O_3 powders were employed to synthesis $Ba_2(In_{1.8}Cr_{0.2})O_5{\cdot}(H_2O)_y$.

In FT-IR spectra of $Ba_2In_2O_5{\cdot}(H_2O)_x$ and $Ba_2(In_{1.8}Cr_{0.2})O_5{\cdot}(H_2O)_y$, the peaks at 871 and 2981 cm^{-1} are assigned to the vibrations of InO_4 tetrahedra units and OH- stretching, respectively The peak at 1416 cm^{-1} is interpreted as the C=O vibration of carbonate. It can be seen that for $Ba_2(In_{1.8}Cr_{0.2})O_5{\cdot}(H_2O)_y$ the peaks at 871 and 2980 cm^{-1} are significantly smaller, whereas the peak at around 1416 cm^{-1} is more pronounced compared to the pristine $Ba_2In_2O_5{\cdot}(H_2O)_x$. Additionally,

characteristic small peaks of $Ba_2In_2O_5{\cdot}(H_2O)_x$ in the wavenumber range of 1250 to 1050 cm^{-1} (small arrows), completely vanished by Cr substitution. In particular, the in XRD Pattern the absence of peaks at 15.5 ° and 21.6 ° suggests a crystal structure with higher symmetry, and form a tetragonal phase.

2.3. Fabrication of perovskite solar cell

Materials for fabrication of solar cells: FTO (Fluorinated-doped Tin Oxide) glass sheets with (15 Ω/square. Device fabrication: FTO coated glass substrates were cut into 1.5×1.5 cm sizes. One piece of the FTO glass was etched by Zn powder in 6 M HCl solution. Then sonicated in soap and water solution, DI water, acetone, a diluted solution of HCl, and isopropanol for 10 min respectively, and then dried in oven 500 °C for one hour. To form a thick TiO_2 blocking layer, diluted titanium isopropoxide solution in ethanol, spin-casted (1000 r.p.m, 30 sec) onto FTO substrated. They were followed by annealing at 500 °C for one hour. A mesoporous TiO_2 layer (m-TiO_2) was deposited by spin coating for (4000 r.p.m, 20 sec). The substrate was immediately and quickly annealed at 100 °C for 10 min, in the following sintered at 450 °C for 30 min. Perovskite precursor with $CH_3NH_3PbI_3$ formula obtained by 462 mg PbI_2, and 159 mg CH_3NH_3I in 1mL mixed solvent of DMF: DMSO = 4:1 (volume ratio), with solvent engineering techniques were deposited by spin–coating (4500 r.p.m, 30 sec). During spin-coating, diethyl ether (150 µL) was poured on the spinning substrate each 12 seconds. [7] Then, the substrated annealed at 100 ºC for 10 min. Subsequently, the hole transport layer, Spiro-MeOTAD, was deposited by spin-coating (3000 r.p.m, 30 sec). Finally, Au was evaporated on the top of the perovskite to produce a completed PSC device.

3. Results and Discussion

In this work, $Ba_2In_2O_5{\cdot}(H_2O)_x$ and $Ba_2(In_{1.8}Cr_{0.2})O_5{\cdot}(H_2O)_y$ employed as additives in a one-step spin-coating deposition method with solvent engineering technique to prepare the perovskite layer, and solar cell device. The $CH_3NH_3PbI_3$ perovskite absorber layers was synthesized with various amount of additive (0.0, 6.2, and 12.4 mg/mL) and perovskite solar cells was fabricated with the FTO/C-TiO_2/Meso-TiO_2/ $CH_3NH_3PbI_3$ /Au arrangement.

3.1. Characterization of prepared PSCs

$CH_3NH_3PbI_3$ solutions with acceptable amounts of additives than others were prepared. Then, the device was fabricated and that performance was studied and shown in Figure 1, and Table 1. The solar cells fabricated without additive (pristine) has the lower open-circuit voltage (V_{oc}) and power-conversion efficiency (PCE), which adopted to result of XRD and SEM that are discussed below, another hand by adding additives in perovskite solution ($CH_3NH_3PbI_3$ in DMF and DMSO), the PCE of solar cell is improved because V_{oc} and fill factor (FF) are increased. Maybe one reason due to the structure properties of inorganic materials with perovskite structural, and the presence of MOFs, which can help to light harvesting. Among them the devices with 5 wt. % of additive displayed better J-V results than others, (Figure 1a). Figure 1b shows IPCE spectra of perovskites prepared with and without additives. The device containing additives displayed broader and improved IPCE spectra from 370 to 800 nm, relative to that prepared without additives. The IPCE spectra of the top-performing compound II reached over 95 %, whereas that of the device prepared without additives was 80 %. The improvement in IPCE spectra is mainly due to the better morphology and crystallinity of the perovskite film. In addition, IPCE spectra of devices showed the different photocurrent generation that confirmed the effects of additives and improvement in exciting band gaps of perovskite structure for harvesting of light.

FE-SEM was applied to investigation of surface morphology of perovskite film, (Figure 2). FE-SEM shows some pinholes in pristine film, and particles are irregular distribution while in Figure 2b, and 2c the particles were almost regular agglomerated with less pinholes. In Figure 3a, 3b, EDX analysis of perovskite layers clearly shows the existence of Barium, Indium, and Chromium in perovskite layers and confirms the presence of elements. For more study in layers, X-ray diffraction (XRD) was used to measure crystallinity and phase purity. XRD pattern of pristine film is shown in Figure 4. The diffraction peak at 2θ: 14.2 °, 20.02 °, 24.5 °, 28.5 °, 31.9 °, and 41.6 ° assigned to (110),

(200), (202), (220), (310), and (400) peaks for tetragonal crystal of CH3NH3PbI3 films. Other peaks at 26.5, 37.9, 45.5 and 51.7 have corresponded to the FTO layer. All of XRD patterns are shown in Figure 4a (pristine), 4b, 4b (2 wt. % Ba2In2O5·(H2O)x), and 4c (2 wt. % Ba2(In1.8Cr0.2)O5·(H2O)y) exhibit one phase with different intensity of some peaks, for example the peak at 2θ=12.6 is appeared due to decomposition of CH3NH3PbI3 and converting to PbI2 (Eq. 1)[29].

$PbI_2\,(s) + CH_3NH_3I\,(aq) \rightleftarrows CH_3NH_3PbI_3\,(s)$ (1)

In $CH_3NH_3PbI_3$ layer, the intensity of peak PbI_2 is significant, which indicant a further degradation of $CH_3NH_3PbI_3$ layer, in comparison to with $CH_3NH_3PbI_3$ with additives. Finally, in the perovskite layer which contains additives, this peak disappears completely. These results show a positive effect of additives on the stability of the perovskite layer against the ambient condition, which can indicate that by using the additives the stability of layers is improved.

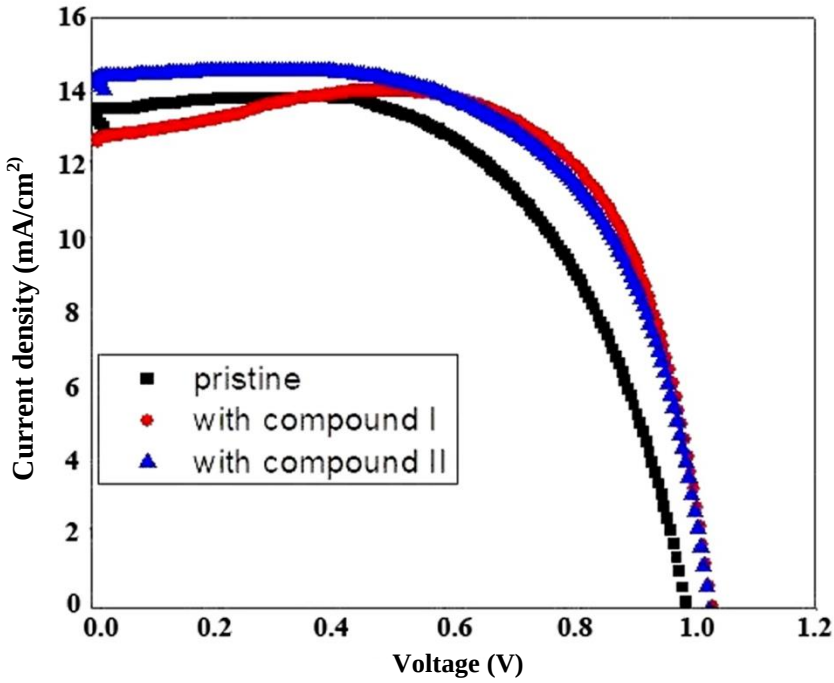

Figure 1: J-V curves of $CH_3NH_3PbI_3$ PSC devices with or without additive measured under illumination of an AM 1.5 solar simulator (100 mW cm^{-2}) in air. The scanning direction is from open-circuit voltage to short circuit. $Ba_2In_2O_5\cdot(H_2O)_x$ (compound I), and and $Ba_2(In_{1.8}Cr_{0.2})O_5\cdot(H_2O)_y$ (compound II), IPCE spectra of $CH_3NH_3PbI_3$ PSC devices with or without additive.

Table1: Photovoltaic properties of prepared cells.

No	Additive in perovskite precursor solution	J_{sc} [mA/cm^2]	V_{oc} [V]	*FF*	η [%]	η after 20 days [%]
I	0 wt % of additive	13.4	0.99	0.59	7.8	3.4
II	2 wt % of compound I	12.6	1.03	0.75	9.7	3.9
III	2 wt % of compound II	14.3	1.02	0.64	9.3	4.9

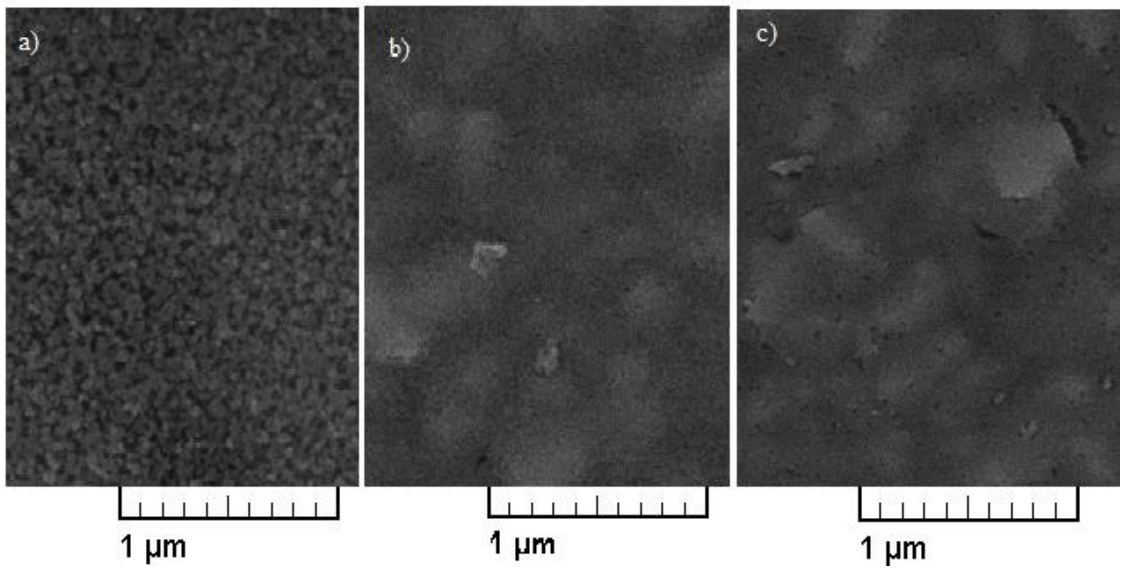

Figure 2: FESEM micrograph of the a) $CH_3NH_3PbI_3$ without additive (pristine perovskite film), b) with 2 wt. % of $Ba_2In_2O_5{\cdot}(H_2O)_x$ (compound I) and c) with 2 wt. % of $Ba_2(In_{1.8}Cr_{0.2})O_5{\cdot}(H_2O)_y$ (compound II).

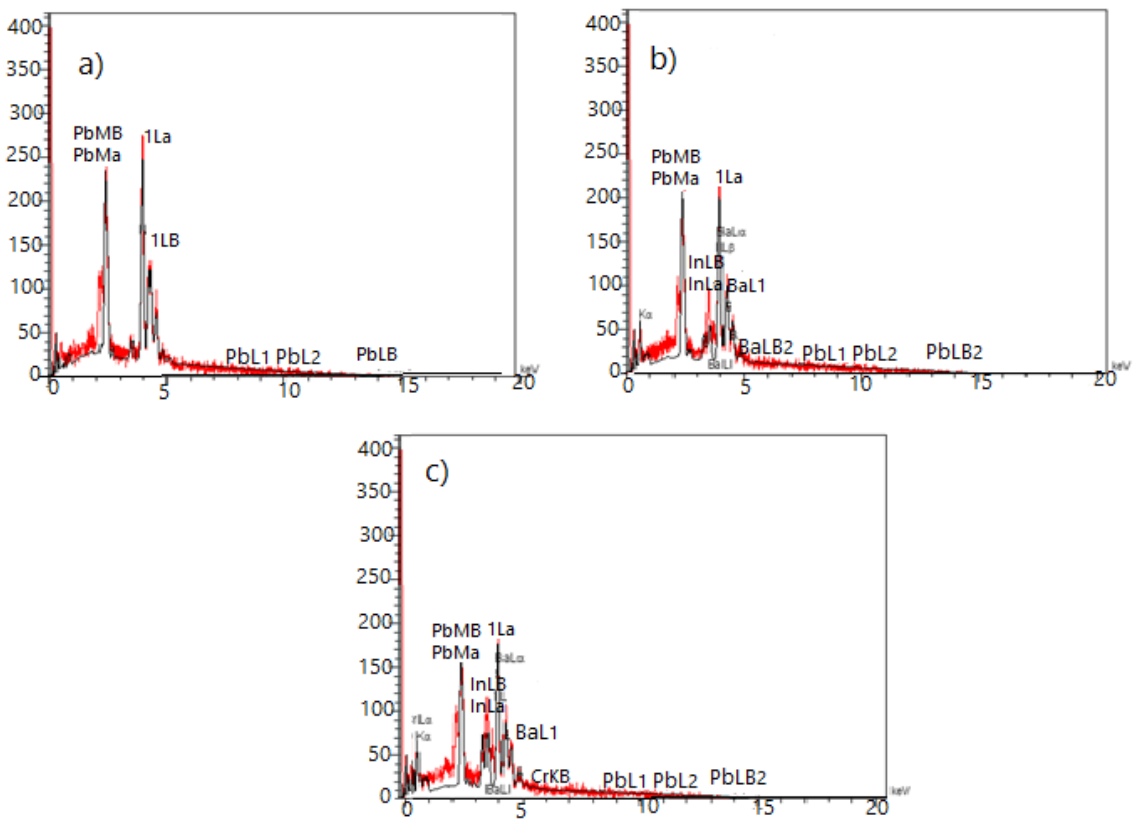

Figure 3: EDX analysis of a) pristine perovskite layer b) perovskite layer with $Ba_2In_2O_5{\cdot}(H_2O)_x$ (compound I) and c) perovskite layer with $Ba_2(In_{1.8}Cr_{0.2})O_5{\cdot}(H_2O)_y$ (compound II).

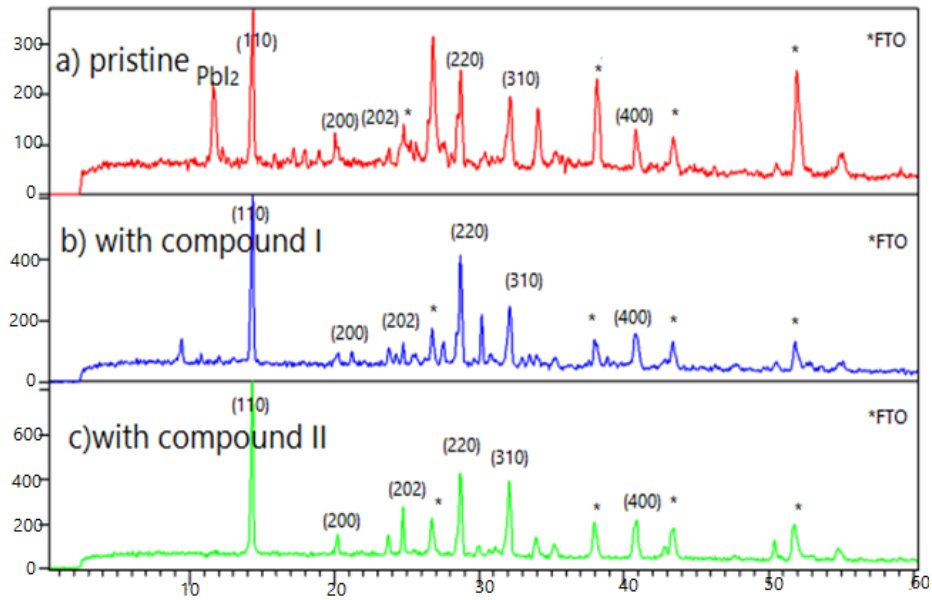

Figure 4: The X-ray powder diffraction pattern of a) $CH_3NH_3PbI_3$ film without additive (pristine perovskite film), b) with 2 wt. % of $Ba_2In_2O_5{\cdot}(H_2O)_x$ (compound I), c) with 2 wt. % of $Ba_2(In_{1.8}Cr_{0.2})O_5{\cdot}(H_2O)_y$ (compound II).

From the most intense (110) peaks the average crystallite size of the layer was estimated using the Sherrer equation [30]. The calculated crystallite size show 49.4 (for pristine), 67.5 (for 2 wt. % of $Ba_2In_2O_5{\cdot}(H_2O)_x$), 66.4 (for 2 wt. % of $Ba_2(In_{1.8}Cr_{0.2})$ $O_5{\cdot}(H_2O)_y$) as additive. As a result, large-crystal- size perovskite formed in the presence of additives [31]. The grain size of crystals increases the quality of perovskite film and can improve the performance of solar cells. These results are adopted to FE-SEM images. The $CH_3NH_3PbI_3$ absorber layers with the various additive amount (0, 12.4 mg/mL) and perovskite solar cells with the FTO/C-TiO_2/Meso-TiO_2/$CH_3NH_3PbI_3$with or without additives, structure were fabricated and used for UV-Vis test. Figure 5 exhibits the absorption of $CH_3NH_3PbI_3$ film with different amounts of additives. The optical absorbance by adding 2 wt. % of additives in perovskite solution shows better absorption. It indicates the optical field in perovskite film due to better surface coverage is increased. Moreover, the color of solution changed and orange color is formed. Thus the absorption of films in visible spectra are changed. The intensities of absorption signal is decreased in the order $Ba_2(In_{1.8}Cr_{0.2})O_5{\cdot}(H_2O)_y$ > $Ba_2In_2O_5{\cdot}(H_2O)_x$ >pristine. The powder color changed the color of $CH_3NH_3PbI_3$ solution from yellow to red in the presence of $Ba_2In_2O_5{\cdot}(H_2O)_x$, and $Ba_2(In_{1.8}Cr_{0.2})O_5{\cdot}(H_2O)_y$. The absorption curve covered a wide range of wavelengths from visible to the near-infrared. In the absorption spectra, the excitation peak appears between 400 to 450 nm, and the onset of absorption is in the range of 700-800 nm. It is observed in Figure 5 that the absorption onset shifts towards the longer wavelength region with adding additives. Because of the increased grain size of the perovskite layer, the absorption onset shifts towards the longer wavelength region. When the perovskite precursors were fabricated with additives, the absorption in range 400-800 nm was very similar. A higher absorption for longer wavelength (> 550 nm) is calculated for samples that made by additives, because of larger grain size that enforces more significant scattering and in addition to that absorption. However, higher optical absorption is measured for perovskite film that fabricated with additives, which is consisted of SEM result indicating. In addition, Cr substitution in $Ba_2In_2O_5{\cdot}(H_2O)_x$ lead to a reduction of the slope of the absorption and a slight increase of the absorption.

UV-Vis absorption was also used to check the band gap. As a result, the amount of band gaps for pristine, and cells with additives obtained 1.1-1.3 ev respectively (Figure 6). Therefore, in the presence of Barium, Indium, and Chromium metals, the band gap of perovskite layer is decreased. This calculation was performed with the Tauck equation (Eq. 2).

$$(\alpha h\nu)=B(h\nu - Eg)^{\frac{n}{2}} \quad (2)$$

In this formula, α is absorption coefficient, B is constant absorption, hν is Stimulation energy, Eg is Band gap energy, and n is constant number which is one for direct transfer, and four for indirect transfer.

Absorption coefficient was calculated using the following formula (Eq. 3).

$$\alpha=2/0303\times 10^{3}\ \left(\frac{AP}{LC}\right) \quad (3)$$

In this formula, α is absorption coefficient, L is optical path length, A is sample adsorption amount in UV-Vis, C is sample molar concentration, and *P* is density [32, 33].

Figure 7 shows the Nyquist plots of electrochemical impedance spectroscopy of perovskite solar cells with and without additives under AM1.5 sun illumination. The resistance of perovskite layers decreases in the presence of additives compare to pristine layer that is indication of better performance and probably less recombination reactions of cells containing additives, or improving the morphology of perovskite layers of solar cells with additives as a result of reducing defects and holes in them.

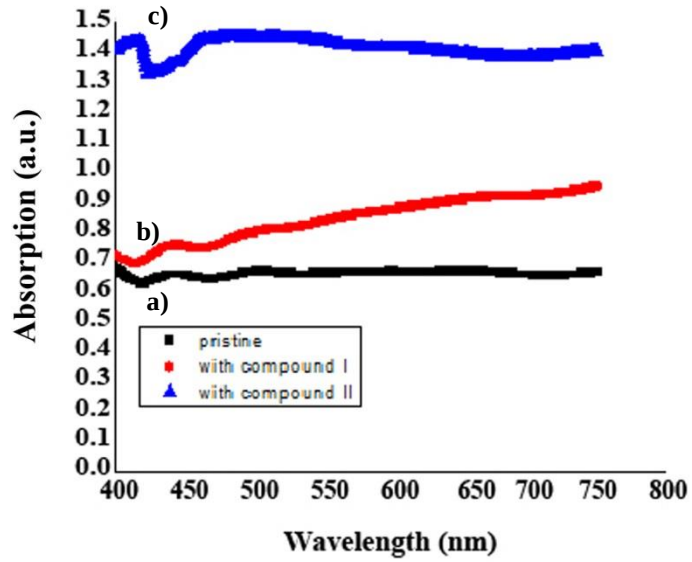

Figure 5: UV-Vis absorption spectra of a) pristine perovskite film b) with 2 wt % of $Ba_2In_2O_5\cdot(H_2O)_x$ (compound I), c) with 2 wt. % of $Ba_2(In_{1.8}Cr_{0.2})O_5\cdot(H_2O)_y$ (compound II).

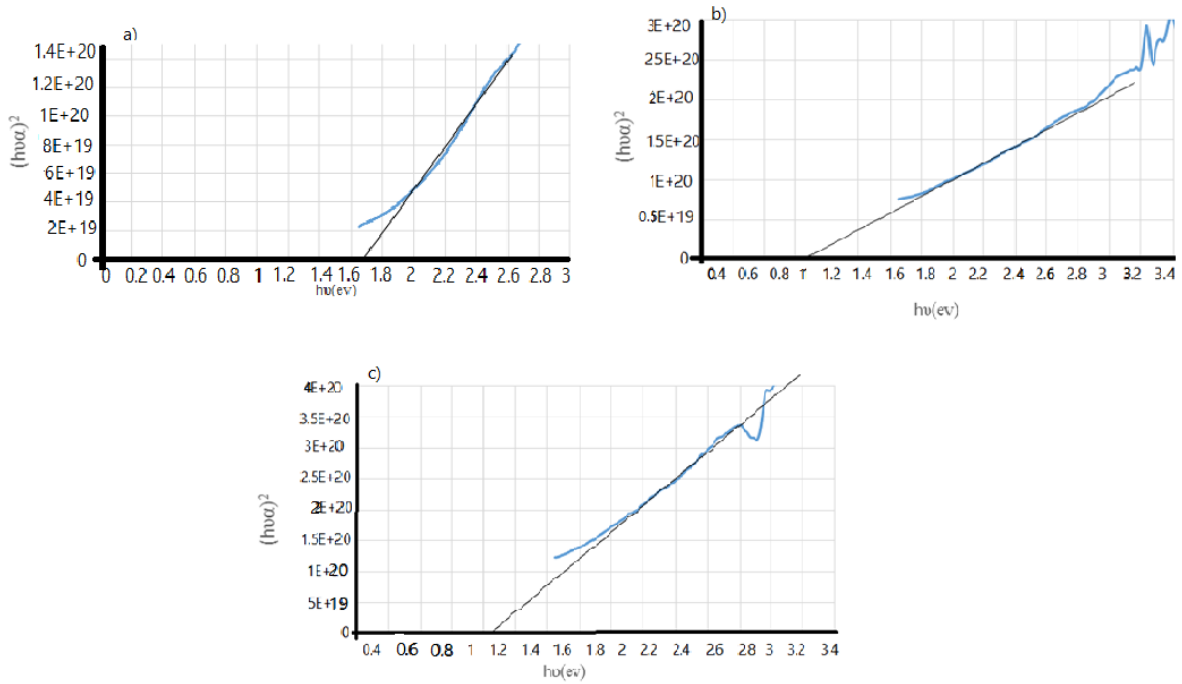

Figure 6: Band gap comparation of a) pristine perovskite film b) with 2 wt. % of $Ba_2In_2O_5\cdot(H_2O)_x$ (compound I), c) with 2 wt. % of $Ba_2(In_{1.8}Cr_{0.2})O_5\cdot(H_2O)_y$ (compound II).

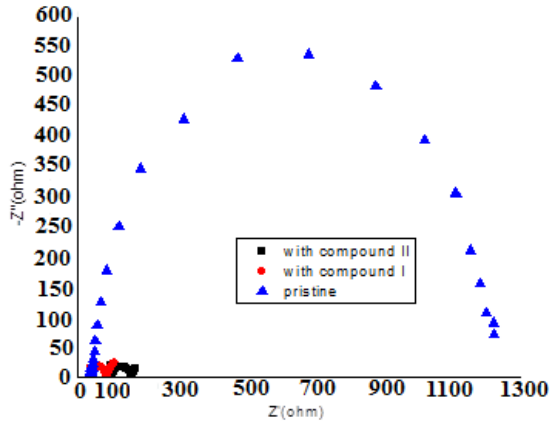

Figure 7: Nyquist plots of pristine perovskite film, with 2 wt. % of $Ba_2In_2O_5{\cdot}(H_2O)_x$ (compound I), and with 2 wt. % of $Ba_2(In_{1.8}Cr_{0.2})O_5{\cdot}(H_2O)_y$ (compound II).

4. Conclusion

The $Ba_2In_2O_5{\cdot}(H_2O)_x$ and $Ba_2(In_{1.8}Cr_{0.2})O_5{\cdot}(H_2O)_y$ perovskite compounds were used as additives in perovskite precursor solution of $CH_3NH_3PbI_3$ by one-step spin-coating method with anti-solvent technique to improve the performance of perovskite solar cells. After fabrication of the PCSs, the device efficiencies increased from 7.8 % to 9.7 %, and 7.8 % to 9.3 % for cells containing additives. XRD patterns of perovskite layers after addition of Cr-substituted and pristine $Ba_2In_2O_5{\cdot}(H_2O)_x$ showed the stability of devices improved because the peaks of perovskite destruction was removed in the presence of the additives. Moreover, this can be due to the improvement of crystal structure and the quality of perovskite layer. On the other, the materials with perovskite structure such as Cr-substituted and pristine $Ba_2In_2O_5{\cdot}(H_2O)_x$ are better able to communicate with the $CH_3NH_3PbI_3$ and TiO_2 and facilitating electron transfer. Finally, the results of this research indicate that the use of Cr-substituted and pristine $Ba_2In_2O_5{\cdot}(H_2O)_x$ additive in perovskite precursor solution is a suitable way for designing and fabrication of stable perovskite solar cells with considerable efficiency.

Acknowledges

The authors are grateful to Dr Yoon Song Hak and Prof. Dr Anke weidenkaff for their useful information and the Iranian Research Organization for Science and Technology (IROST).

5. References

1. S. De Wolf, J. Holovsky, S.J. Moon, P. Löper, B. Niesen, M. Ledinsky, F.J. Haug, J.H. Yum, C. Ballif, Organometallic halide perovskites: sharp optical absorption edge and its relation to photovoltaic performance, *J. Phys. Chem. Let.*, 5(2014), 1035-1039.
2. G.E. Eperon, S.D. Stranks, C. Menelaou, M.B. Johnston, L.M. Herz, H.J. Snaith, Formamidinium lead trihalide: a broadly tunable perovskite for efficient planar heterojunction solar cells, *Energ Environ. Sci.*, 7(2014), 982-988.
3. C. R. Kagan, D. B. Mitzi, and C. D. Dimitrakopoulos, Organic-inorganic hybrid materials as semiconducting channels in thin-film field-effect transistors, *Sci.*, 286(1999), 945-947.
4. S.D. Stranks, G.E. Eperon, G. Grancini, C. Menelaou, M.J. Alcocer, T. Leijtens, L.M. Herz, A. Petrozza, H.J. Snaith, Electron-hole diffusion lengths exceeding 1 micrometer in an organometal trihalide perovskite absorber, *Sci.*, 342(2013), 341-344.
5. I.m. JH, I.H. Jang, N. Pellet, M. Grätzel, N.G. Park, Growth of $CH_3NH_3PbI_3$ cuboids with controlled size for high-efficiency perovskite solar cells, Nat. Nanotechnol., 9(2014), 927.
6. W. Nie, H. Tsai, R. Asadpour, J.C. Blancon, A.J. Neukirch, G. Gupta, J.J. Crochet, M. Chhowalla, S. Tretiak, M.A. Alam, H.L. Wang, High-efficiency solution-processed perovskite solar cells with millimeter-scale grains, *Sci.*, 347(2015), 522-526.
7. N.J. Jeon, J.H. Noh, Y.C. Kim, W.S. Yang, S. Ryu, S.L. Seok, Solvent engineering for high-performance inorganic-organic hybrid perovskite solar cells, *Nat. Mater.*, 13(2014), 897-903.
8. T. Li, Y. Pan, Z. Wang, Y. Xia, Y. Chen, W. Huang, Additive engineering for highly efficient organic – inorganic halide perovskite solar cells : recent advances and perspectives, *J. Mater. Chem. A.*, 5(2017), 12602-12652.
9. M.P. Suh, H.J. Park, T.K. Prasad, D.W. Lim, Hydrogen

storage in metal–organic frameworks, *Chem. Rev.*, 112(2012), 782-835.
10. Li. JR, J. Sculley, HC. Zhou, Metal a organic frameworks for separations, *Chem. Rev.*, 112 (2012), 869-932.
11. L.E. Kreno, K. Leong, O.K. Farha, M. Allendorf, R.P. Van Duyne, J.T. Hupp, Metal organic framework materials as chemical sensors, *Chem. Rev.*, 112(2012), 1105-1125.
12. L. Ma, J.M. Falkowski, C. Abney, W. Lin, frameworks as a tunable platform for asymmetric catalysis, Nat. Chem., 2(2010), 838-846.
13. J. Lee, OK. Farha, J. Roberts, KA. Scheidt, ST. Nguyen, JT. Hupp, Metal – organic frameworks issue Metal – organic framework materials as catalysts, *Chem. Soc. Rev.*, 38(2009), 1450-1459.
14. P. Mahata, G. Madras and S. Natarajan, Novel photocatalysts for the decomposition of organic dyes based on metal-organic framework compounds, *J. Phys. Chem. B.*, 110(2006), 13759-13768.
15. L. L Wen, F. Wang, J. Feng, K. L. Lv, C. G. Wang and D. F. Li, Structures, photoluminescence, and photocatalytic properties of six new metal-organic frameworks based on aromatic polycarboxylate acids and rigid imidazole-based synthons, *Cryst. Growth. Des.*, 9(2009), 3581-3589.
16. C. Wang, Z. Xie, K. E. deKrafft and W. Lin, Doping metal-organic frameworks for water oxidation, carbon dioxide reduction, and organic photocatalysis, *J. Am. Chem. Soc.*, 133(2011), 13445–13454.
17. C. Wang, Z. Xie, K.E. deKrafft and W. Lin, Light-harvesting cross-linked polymers for efficient heterogeneous photocatalysis, *ACS Appl Mater Interfaces.*, 4(2012), 2288-2294.
18. AV. Vinogradov, H. Zaake-Hertling, E. Hey-Hawkins, AV. Agafonov, GA. Seisenbaeva, VG. Kessler, VV. Vinogradov, The first depleted heterojunction TiO_2–MOF-based solar cell, *Chem. Comm.*, 1(2014), 14-17.
19. D. Shen, A. Pang, Y. Li, J. Dou, M. Wei, Metal-organic frameworks at interfaces of hybrid perovskite solar cells for enhanced photovoltaic, *Chem. Commun.*, 54 (2018), 1253-1256.
20. TH. Chang, CW. Kung, HW. Chen, TY. Huang, SY. Kao, HC. Lu, MH. Lee, KM. Boopathi, CW. Chu, KC. Ho, Planar heterojunction perovskite solar cells incorporating metal-organic framework nanocrystals, *Adv. Mater.*, 27(2015), 7229-7235.
21. M. Li, D. Xia, Y. Yang, X. Du, G. Dong, A. Jiang, R. Fan, Doping of $[In_2(phen)_3Cl_6]CH_3CN\ 2H_2O$ indium-based metal–organic framework into hole transport layer for Eenhancing perovskite solar cell efficiencies, *Adv. Energy Mater.*, 8(2018), 1702052.
22. M. Li, D. Xia, A. Jiang, X. Du, X. Fan, L. Qiu, P. Wang, R. Fan, Y. Yang, Enhanced crystallization and optimized morphology of perovskites through doping an indium based metal-organic assembly: achieving significant solar cell efficiency enhancements, *Energy Technol.*, **7**(2019), 1900027.
23. M.S. Sowmehesaraee, M. Ranjbar, M. Abedi, S.A. Mozaffari, Fabrication of lead iodide perovskite solar cells by incorporating zirconium, indium and zinc metal-organic frameworks, *Sol. Energy*, 214 (2021), 174586.
24. M.S. Sowmehesaraee, M. Ranjbar, M. Abedi, Incorporating MOF-235 in lead iodide perovskite solar cell and investigating its efficiency and stability, *J. Mater. Sci.: Mater. Electron.*, 27(2021), 1-8.
25. M. Seifpanah Sowmehsaraee, M. Ranjbar, M. Abedi, F. Rouhani, A. Morsali, The Effect of Zn (II) Containing MetalOrganic Frameworks on Perovskite Solar Cells, *Prog. Color Colorants Coat.*, 14(2021), 259-267.
26. E. Maleki, M Ranjbar ,S. A. Kahani, Investigating the effect of the delay time of dripping antisolvent on morphology and structure of the perovskite layer and its application in the hole-transport, *Prog. Color Colorant Coat.*,14(2021), 54-47.
27. E. Kouhestanian, M. Ranjbar, A. Mozaffari, H. Salar amoli, Investigation of thickness effects on the performance of ZnO-based DSSC, *Prog. Color Colorant Coat.*,14(2021), 101-112.
28. Y. Song Hak, S. Nikoee, M. Ranjbar, D. Ziegenbalg, M. Widenmeyer, A. Weidenkaff, Strongly affected photocatalytic CO_2 reduction by CO_2 adsorbed to the surface of $Ba_2\ (In_{1.8}Cr_{0.2})\ O_5{\cdot}(H_2O)$ δ powders, *Solid State Sci.*, 105(2020), 106212.
29. X. Guo, C. Mccleese, C. Kolodziej, A. C. S. Samia, Y. Zhao, and C. Burda, intermediate phase in hybrid organic- inorganic, *R. Soc. Chem.*, 45(2016) 3806-3813.
30. W. Zhang, M. Saliba, D.T. Moore, S.K. Pathak, M.T. Hörantner, T. Stergiopoulos, S. D. Stranks Ultrasmooth organic-inorganic perovskite thin-film formation and crystallization for efficient planar heterojunction solar cells, *Nat. comm.*, 6(2015), 1-10.
31. C.Y. Chang, C.Y. Chu, Y.C. Huang, C.W. Huang, S.Y. Chang, C.A. Chen, C.Y. Chao, Su, W.F, Tuning perovskite morphology by polymer additive for high efficiency solar cell, *ACS Appl. Mater. Inter.*, 7(2015), 4955-4961.
32. P. Makuła, M. Pacia, W. Macyk, How to correctly determine the band gap energy of modified semiconductor photocatalysts based on UV–Vis spectra, *J. Phys. Chem. Lett.*, 9(2018), 6814-6817.
33. P.R. Jubu, F.K. Yam, V.M. Igba, Tauc-plot scale and extrapolation effect on bandgap estimation from UV–vis–NIR data–a case study of β-Ga_2O_3, *J. Solid State Chem.*, 290(2020), 121576.

How to cite this article:
M. Seifpanah Sowmehsaraee, M. Ranjbar, M. Abedi, Fabrication of lead Iodide perovskite solar cells by incorporating Cr-substituted and pristine $Ba_2In_2O_5{\cdot}(H_2O)$x as additives. Prog. Color Colorants Coat., 16 (2023), 21-29.